HHS Public Access

Author manuscript

Metabolomics. Author manuscript; available in PMC 2016 August 01.

Published in final edited form as:

Metabolomics. 2015 August 1; 11(4): 895–907. doi:10.1007/s11306-014-0747-6.

Untargeted metabolomics studies employing NMR and LC-MS reveal metabolic coupling between *Nanoarcheum equitans* and its archaeal host *Ignicoccus hospitalis*

Timothy Hamerly[1,ζ], **Brian P. Tripet**[1,ζ], **Michelle Tigges**[1,ζ], **Richard J. Giannone**[3], **Louie Wurch**[3,4], **Robert L. Hettich**[3], **Mircea Podar**[3,4], **Valerie Copié**[1,2,*], and **Brian Bothner**[1,2,*]

[1]Department of Chemistry and Biochemistry, Montana State University, Bozeman, MT 59717

[2]Thermal Biology Institute, Montana State University, Bozeman, MT 59717

[3]Oak Ridge National Laboratory, Oak Ridge, TN 37831

[4]Department of Microbiology, University of Tennessee, Knoxville, TN 37996

Abstract

Interspecies interactions are the basis of microbial community formation and infectious diseases. Systems biology enables the construction of complex models describing such interactions, leading to a better understanding of disease states and communities. However, before interactions between complex organisms can be understood, metabolic and energetic implications of simpler real-world host-microbe systems must be worked out. To this effect, untargeted metabolomics experiments were conducted and integrated with proteomics data to characterize key molecular-level interactions between two hyperthermophilic microbial species, both of which have reduced genomes. Metabolic changes and transfer of metabolites between the archaea *Ignicoccus hospitalis* and *Nanoarcheum equitans* were investigated using integrated LC-MS and NMR metabolomics. The study of such a system is challenging, as no genetic tools are available, growth in the laboratory is challenging, and mechanisms by which they interact are unknown. Together with information about relative enzyme levels obtained from shotgun proteomics, the metabolomics data provided useful insights into metabolic pathways and cellular networks of *I. hospitalis* that are impacted by the presence of *N. equitans*, including arginine, isoleucine, and CTP biosynthesis. On the organismal level, the data indicate that *N. equitans* exploits metabolites generated by *I. hospitalis* to satisfy its own metabolic needs. This finding is based on *N. equitans*'s consumption of a significant fraction of the metabolite pool in *I. hospitalis* that cannot solely be attributed to increased biomass production for *N. equitans*. Combining LC-MS and NMR metabolomics datasets improved coverage of the metabolome and enhanced the identification and quantitation of cellular metabolites.

*Correspondence should be addressed to: Drs. Brian Bothner and Valérie Copié, Montana State University, Chemistry & Biochemistry Department, CBB 103, Bozeman, MT 59717, Phone: (406)-994-5270 and (406)-994-7244, bbothner@chemistry.montana.edu and ycopie@chemistry.montana.edu.

ζdenotes that all three authors contributed equally to this work

Conflict of Interest Statement:
The authors declare no conflict of interest

Compliance with ethical requirements:
This article does not contain any studies with human or animal subjects

Keywords

LC-MS; NMR; metabolomics; *Ignicoccus hospitalis*; *Nanoarcheum equitans*; hyperthermophilic Archaea; interspecies interactions; metabolic pathway analysis; systems biology

Introduction

In the environment, microbes do not live in isolation, but rather constantly respond to the presence of other species, adapting their metabolic needs and resources to optimize growth and survival among species that share similar ecological niches. Microbial communities depend on specific and complex mechanisms of interspecies interactions and communications, forming sophisticated interspecies networks ranging from mutualism to symbiosis or parasitism. Such interspecies relationships impact the role of keystone species in an ecological community, play a major role in energy and elemental cycles, and form the foundation of host-pathogen interactions.

Despite a long history of research focused on understanding the molecular mechanisms underlying host-microbe interactions, and the growing interest in identifying microbial metacommunities, fundamental processes of interspecies recognition, interactions, and communication remain unclear. In particular, little is known about the biochemical processes by which mutualism and syntrophy (i.e. metabolic interdependence) impact microbial genome evolution, and how metabolism and energetic coupling between species affect host-microbe homeostasis and their responses to environmental factors. Such a lack of fundamental knowledge is most prevalent for organisms from the Archaeal domain of life, such as *Ignicoccus hospitalis* and *Nanoarchaeum equitans*, which engage in one of the simplest symbiotic/parasitic systems known (Jahn *et al*., 2008; Junglas *et al*., 2008; Podar *et al*., 2008).

The reduced genome complexity of *I. hospitalis and N. equitans* is an attractive model for the study of fundamental cellular, genomic, and metabolic principles guiding inter-species interactions, as the genomes of both organisms have been sequenced, a metabolic map of the *Ignicoccus – Nanoarcheum* system has been reconstructed, and some of the biochemical pathways and cellular complexes have been experimentally validated (Huber *et al*., 2008; Huber *et al*., 2003; Jahn *et al*., 2007; Jahn *et al*., 2004; Küper *et al*., 2010; Podar *et al*., 2008; Waters *et al*., 2003).

Ignicoccus is a genus of marine hyperthermophilic, chemolithoautotrophic Archaea, classified to the order Desulfurococcales (Huber *et al*., 2000). These organisms reduce elemental sulfur with hydrogen as a source of energy and use carbon dioxide as the sole carbon source (Jahn *et al*., 2007). *Ignicoccus* species possesses some of the smallest genomes of a free living organism, some having less than 1500 genes (Podar *et al*., 2008). One species of this genus (*Ignicoccus hospitalis*) has been shown to act as a host for one of the smallest organisms known, *Nanoarchaeum equitans*, which encodes approximately 550 proteins. It lacks many of the genes required for energy production and depends exclusively on *Ignicoccus* for survival (Giannone *et al*., 2011; Huber *et al*., 2002; Huber *et al*., 2003; Paper *et al*., 2007). *N. equitans* is a member of the proposed phylum *Nanoarchaeota*, and

currently the only cultivated organism from that group of Archaea (Huber *et al*., 2000; Huber *et al*., 2002).

Investigations of the protein composition of *N. equitans* reveal that it is comprised of a very minimal proteome with important bioenergetic proteins and protein complexes missing or incomplete (Giannone *et al*., 2011, 2014; Waters *et al*., 2003). In addition, *N. equitans* is unable to synthesize many metabolites and lipids on its own, and relies on essential cellular nutrients and metabolic components that are provided via interactions and cell-cell contacts with *I. hospitalis* (Burghardt *et al*., 2009; Huber *et al*., 2012; Jahn *et al*., 2004). Despite these observations, it remains to be established whether *N. equitans* is a parasite or provides an advantage to *I. hospitalis*, as the latter does not seem to benefit or suffer when grown in co-culture with *N. equitan*s (Burghardt *et al*., 2009; Giannone *et al*., 2011; Godde, 2012; Huber *et al*., 2012; Jahn *et al*., 2008, 2004; Junglas *et al*., 2008).

In order to better understand the foundational biochemistry and metabolic networks regulating *I. hospitalis – N. equitans* interspecies interactions, we have undertaken an untargeted mass spectrometry (MS) and nuclear magnetic resonance (NMR) based metabolomics study of this archaeal host-microbe model system. Utilization of both NMR and MS have enabled us to take advantage of the complementarity of the two techniques for metabolomics analysis, and to establish distinct metabolite profiles of *I. hospitalis* alone and when grown in co-culture with *N. equitans*. The metabolomics data thus acquired have been integrated with published genomics and proteomics information using Pathway Tools, to generate a multilevel model of cellular processes (genes, proteins, metabolites) and metabolic networks that regulate *I. hospitalis* and *N. equitans* interactions (Giannone *et al*., 2014; Karp & Paley, 1996; Karp *et al*., 2005, 2010; Karp *et al*., 2002; Paley *et al*., 2012). Results from the global analysis of these multi “omics” data suggest that *N. equitans* exploits metabolites produced by *I. hospitalis* to satisfy its own metabolic needs, while still allowing both organisms to live.

Methods and Materials

Materials

All solvents from metabolite extraction and LC-MS analysis were purchased in HPLC grade; water from Avantor (Center Valley, PA) and methanol and acetonitrile from EMD Chemicals Inc. (Gibbstown, NJ). Formic acid (98% GR ACS) for use as an ion pairing agent was purchased from EMD Chemicals Inc. (Gibbstown, NJ). DSS (4,4-dimethyl-4-silapentane-1-sulfonic acid) used for NMR spectral reference and metabolite quantification was purchased from Sigma. All solvents were used as supplied without further purification.

Cell Culturing

I. hospitalis and *I. hospitalis – N. equitans* were cultured for 24 hours in 1 liter bottles containing 250 ml 0.5X SME medium, sulfur (10g/l) and a H_2-CO_2 (80-20%) gas phase (15 psi), at 85 °C, as described previously (Jahn *et al*., 2008). Prior to harvesting, the cultures were cooled to room temperature, chilled on ice and the cells were collected by centrifugation (8000 xg for 20 minutes). The cell pellets were washed with cold anaerobic

0.5X SME medium, aliquoted in small tubes, and flash frozen with liquid nitrogen under N_2 gas, and stored at −80 °C.

Metabolite Extraction

Intracellular metabolites from *I. hospitalis* and *I. hospitalis – N. equitans* co-cultures for LC-MS and NMR analysis were extracted using a 50% aqueous (v/v) MeOH extraction, modified from a previously published protocol (Heinemann *et al*., 2014). Briefly, frozen cell pellets weighing 50 mg for LC-MS analysis and 115 mg for NMR analysis, were re-suspended in 300 μL of 50% MeOH (v/v), vortexed for 30 seconds, and lysed by sonication for 5 minutes on ice. The resulting samples were then incubated for 1 hour at -20 °C to allow diffusion of metabolites into the bulk liquid. Following this step, cell debris was pelleted by centrifugation for 15 minutes at 20,000 ×g and supernatant was collected. Cell debris was then washed with an additional volume of 50% MeOH (v/v), vortexed for 30 seconds, centrifuged, and supernatant pooled. Proteins were precipitated using 5:1 dilution with cold acetone, left overnight at −80 °C, and centrifuged. The resulting supernatant was collected and dried via vacuum speed concentration, and stored at −80 °C. For LC-MS analysis, metabolite extracts were re-suspended in 50% MeOH.

LC-MS Based Metabolomic Analysis

For reverse phase analysis, a Kinetex 1.7 μm C18 150 mm x 2.1 mm column (Phenomenex, Torrance, CA) kept at 50 °C was used for LC separation with a flow rate of 600 μL min^{-1}. Solvent A consisted of 0.1% formic acid in water, while solvent B was 0.1% formic acid in acetonitrile. The elution gradient consisted of 2% solvent B for 2 minutes (with the first two minutes going to waste to avoid contaminating the source with excess salt), to 95% solvent B over 24 minutes, held at 95% for 2 minutes, and then returned to 2% for 2 minutes, with a total run time of 30 minutes using an Agilent 1290 UPLC (Agilent, Santa Clara, CA) system connected to an Agilent 6538 Q-TOF Mass Spectrometer (Agilent, Santa Clara, CA).

Normal phase analysis used a Cogent Diamond Hydride HILIC 150 mm x 2.1 mm column (MicroSolv, Eatontown, NJ) was used for LC separation with a flow rate of 600 μL min^{-1}. Solvent A consisted of 0.1% formic acid in water, while solvent B consisted of 0.1% formic acid in acetonitrile. The elution gradient consisted of 95% solvent B for 2 minutes (with the first minute going to waste to avoid contaminating the source with excess salt), to 50% solvent B over 24 minutes, held at 50% for 2 minutes, and then returned to 95% for 2 minutes, with a total run time of 30 minutes using an Agilent 1290 UPLC (Agilent, Santa Clara, CA) system connected to an Agilent 6538 Q-TOF Mass Spectrometer (Agilent, Santa Clara, CA).

Mass spectrometry analysis was conducted in positive ion mode, with a cone voltage of 3500V and a fragmentor voltage of 120V. Drying gas temperature was 350 °C with a flow of 12 L min^{-1} and the nebulizer was set to 60 psig. Spectra were collected at a rate of 2.52 per second with a mass range of 50 to 1000 m/z. The mass analyzer resolution was 18,000 and post calibration tests had a mass accuracy of approximately one ppm.

Identification of compounds with retention time matches to standards was strengthened with fragmentation analysis (MS/MS) when possible. LC and MS parameters were the same as listed above. For MS/MS acquisition, both standard compounds and ions of interest from the samples were selected in a window of ±1.7 m/z units, and fragmented at 10V and 20V.

LC-MS Data Processing and Analysis

Data files from the LC-MS were converted to .MZxml format using the Masshunter Qualitative software provided with Agilent instruments (Agilent, Santa Clara, CA). Analysis of LC-MS data was done using the software package MZmine (version 2.10). Procedures, together with parameters used for the alignment of features and identification in MZmine, were as follows: LC-MS files were imported into MZmine, followed by data set filtering to remove the first minute of elution data for HILIC analysis, and the first two minutes of elution data for RP analysis. A minimum intensity cutoff of 5000 and a minimum elution time window of 0.1 minutes were used to create molecular feature lists. Lists included retention time (R/T) adjusted with a tolerance of 0.2 minutes or less. These R/T-adjusted lists were then aligned into one mass list, and then gap-filled to add missing peaks not detected in all runs with an m/z tolerance of 15.0 ppm. Identification of compounds was based on annotated pathways in Biocyc, or standard compounds based on R/T and m/z was done on these finalized lists with an m/z tolerance of 30 ppm and for the standards a retention time tolerance of 0.25 minutes (Karp *et al*., 2005, 2002). Metabolite identities were each manual annotated to ensure strong matches, tandem mass spectrometry was done to further confirm metabolite ID. Lists of aligned and R/T adjusted molecular features were analyzed using principal component analysis (PCA) using the XLSTAT software package (Addinsoft 2013). Ions selected for MS/MS identification were confirmed by matching fragmented peaks and intensities to those of the standard compounds.

NMR Based Metabolomic Analysis and Data Processing

For ^{1}H 1D NMR, duplicate metabolite samples were resuspended in 200 μL of NMR buffer (10mM NaH_2PO_4/ Na_2HPO_4 containing 0.25 mM 4,4-dimethyl-4-silapentane-1-sulfonic acid (DSS) in 100% D_2O, pH 7) and transferred to a 5 mm Shigemi high-salt tolerant NMR tube (Shigemi Inc.). ^{1}H NMR spectra were acquired at 298K (25°C) on a Bruker 600-MHz (^{1}H Larmor frequency) AVANCE III solution NMR spectrometer equipped with a SampleJet automatic sample loading system, a 5 mm triple resonance (^{1}H, ^{15}N, ^{13}C) liquid helium-cooled TCI probe (cryoprobe™), and Topspin software (Bruker version 3.2). One-dimensional ^{1}H NOESY experiments were performed using the Bruker supplied noesypr1d pulse sequence with 256 scans, ^{1}H spectral window of 9600 Hz. FIDS were collected in 32K time data points, with a dwell time interval of 52 μsec between points amounting to an acquisition time of ~ 1.7 sec, using a 2 second relaxation recovery time delay between FID acquisitions, and a NOESY mixing time period of 50 msec. Pulse sequence settings were based on standard recommendations by the Chenomx™ user guide for recording 1D ^{1}H NMR spectra of small molecules and for quantitation of metabolites.

Spectral processing and analysis was performed using the Chenomx™ software (version 7.6) (Chenomx Inc., Edmonton, AB, Canada). For each sample, NMR spectra were phased, baseline corrected, and a line broadening function of 0.5 Hz was applied, following

recommended Chenomx protocols and previously reported metabolomics analysis methods (Sun *et al*., 2012; Tredwell *et al*., 2011; Weljie *et al*., 2006; Wu *et al*., 2010). For metabolite identification, the Chenomx small molecule library for 600-MHz (^{1}H Larmor frequency) magnetic field strength NMR spectrometers was used, and NMR spectral patterns were fitted for each sample independently. Metabolite identifications were further confirmed by analysis of 2D ^{1}H-^{1}H total correlation spectroscopy (TOCSY) spectra or by spiking, when available, pure metabolite standards into the samples. An internal DSS standard was used for quantitation of identified metabolites. Equivalent weight cell pellets were used to prepare the NMR samples and post data acquisition and metabolite profiling analysis, NMR spectra were normalized based on protein concentration in the insoluble and soluble pellet fractions as determined by SDS-PAGE analysis. This added normalization step corrected for a significant presence of inorganic sulfur present in the pellet of the *I. hospitalis – N. equitans* co-culture, and the inability to obtain direct cell counts from cell pellets provided for metabolomics analysis.

Pathway Tools Analysis of Overlayed Metabolomic and Proteomic Datasets

Using the Pathway Tools v17.5 software (SRI International), NMR and LC-MS metabolite identities and abundances were overlaid with previously published proteomics datasets for *I. hospitalis* only cultures and *I. hospitalis – N. equitans* co-cultures (Giannone *et al*., 2011,2014; Karp & Paley 1996; Karp *et al*., 2005, 2010, 2002; Paley *et al*., 2012). Metabolite identities and their associated fold changes were overlaid onto the IHOS453591 Cyc version 17.0 database, which is available directly from the Biocyc webservers (Karp *et al*., 2005, 2002). The constructed pathway tools database was further curated and adjusted based on analysis of the published literature on *I. hospitalis* and *N. equitans*.

Firefly Luciferase Assay for Quantitation of ATP

Determination of ATP concentrations in both cultures was carried out using the BacTiter-Glo Firefly Luciferase Assay (Promega, Madison, WI) following the protocol included with the kit (Promega Corporation 2012). Briefly, BacTiter-Glo buffer and BacTiter-Glo substrate were equilibrated to room temperature. Substrate was then re-suspended in 10 mL buffer with gentle vortexing to form the BacTiter-Glo reagent. To perform the ATP measurements, 6.5 mg of *I. hospitalis* and *I. hospitalis – N. equitans* co-culture cell pellets were re-suspended in 100 μL of H_2O, and placed into a white 96-well plate. Cells in solution were allowed to equilibrate to room temperature, and then an equal volume (100 μL) of BacTiter-Glo reagent was added to each well with cells, as well as to a well containing 100 μL of H_2O only to serve as a blank. A standard curve of ATP concentrations was generated from 1 μM to 10 pM from a 1 μM stock solution and mixed with BacTiter-Glo reagent and also placed in the same white 96-well plate. The plate was placed on an orbital shaker (Thermoscientific) for five minutes to assist with cell lysis. Luminescence readings for the assay were recorded on a Fluoroskan Ascent FL Microplate Luminometer (Thermo Fisher Scientific Inc., Waltham, MA) and data processing of data was accomplished using the Ascent Software.

Results and Discussion

LC-MS Based Metabolomics Analysis

Metabolite extracts of *I. hospitalis* cells grown alone and in co-culture with *N. equitans* were analyzed using liquid chromatography-mass spectrometry (LC-MS). Three independent biological replicates were used for each type of cell culture. Differential analysis based on molecular feature intensity was used to compare sample groups. Figure 1A presents a cloud plot of reverse phase LC-MS metabolite data from *I. hospitalis* alone and in co-culture with *N. equitans*. Red circles indicate MS spectral features that are in greater abundance when *I. hospitalis* is grown alone, while green circles indicate features that are in greater abundance in the *I. hospitalis – N. equitans* co-culture. The size of the circle indicates fold change between cultures and the shade of each color indicates *p*-value, whereby larger, darker circles signify greater fold change and more significant *p*-values. A number of differences between cultures were observed from these data. Greater than 3000 molecular MS spectral features were detected between the 6 samples, with approximately 100 features being significantly distinct between groups (i.e. exhibiting fold changes greater than 1.5 and a *p*-value less than 0.01). The vast majority of metabolite changes corresponded to decreases in metabolite abundance in the *I. hospitalis – N. equitans* co-cultures. Figure 1B displays the results from a principal component analysis (PCA) of molecular features identified from *I. hospitalis* and co-culture samples (in triplicate). This figure indicates that *I. hospitalis*-only cultures and *I. – hospitalis N. equitans* co-cultures clearly separate from each other along the first principal component (PC1) axis, with PC1 and PC2 accounting for ~ 71% of the variance between cultures. A Venn diagram of molecular features found exclusively in *I. hospitalis* or in co-culture samples, as well as the number of molecular features found in both sets of samples, is shown in Figure 1C.

As a large number of molecular features were observed, data reduction was undertaken to tease out biologically interesting metabolites from the LC-MS metabolomics experiments. Two main data reduction strategies were conducted: First, a small in-house database of prominent and microbial-relevant compounds was created and annotated using retention times and masses (m/z ratios) of authentic standards. This database enabled positive identification of compounds based on both accurate mass and retention time characteristics. As establishing an exhaustive library of standards for all putative compounds is not practical, additional data reduction was conducted to further mine the data for biologically interesting compounds. Specifically, metabolites that are biologically relevant to the *I. hospitalis – N. equitans* system were highlighted by matching molecular masses within a 20 ppm mass error range to a list of expected compounds based on curated genome annotation via the Biocyc pathway tools software (*Karp et al*., 2010).

Metabolites identified via MS standards and pathway analysis of the LC-MS data are displayed in the first four columns of Table 1. A fold change was calculated for each metabolite identified, where a positive number denotes a higher concentration when *I. hospitalis* is grown alone, and a negative fold change indicates a higher concentration in the *I. hospitalis – N. equitans* co-cultures. A total of 39 compounds were putatively identified from the LC-MS analysis by matching MS molecular features with predicted compounds

based on genome annotation or by matching features to MS standards based on retention time and accurate mass measurements. The metabolite identities shown in Table 1 represent strong matches and are expected to be present based on what is known about *I. hospitalis* and *N. equitans* metabolic networks (e.g. amino acids and nucleotides). Of the 39 putatively identified molecules, 21 were confirmed by accurate mass and retention time match to authentic standards. Eight of these were further confirmed by tandem mass spectrometry (MS/MS), as indicated in Table 1. An example of how the metabolite ID of arginine was confirmed by MS/MS is included in supplementary Figure S1. Several sugars including maltotriose and stachyose had excellent m/z and retention time matches to standards, but could not be confirmed with MS/MS due to low abundance in the samples. The presence of such sugars is somewhat unexpected as metabolic pathways involving these molecules have not yet been annotated in *I. hospitalis* or *N. equitans* (Huber *et al*., 2012).

NMR Based Metabolomics Analysis

Analysis of metabolites by NMR is highly complementary to metabolite profiling by LC-MS. In addition to confirming putative metabolite identities from LC-MS, NMR yields quantitative information on metabolite concentrations, and is able to detect molecules that are not typically observed by LC-MS. Representative 1D ^{1}H NMR spectra obtained from metabolite extracts of *I. hospitalis* grown alone (Figure 2A), and in co-culture with *N. equitans* (Figure 2B) show the rich spectral information of the samples. A total of 55 metabolites were identified from analysis of the 1D ^{1}H NMR spectra of *I. hospitalis* and *I. hospitalis – N. equitans* cultures, by matching NMR spectral patterns to reference metabolite spectra included in the 600 MHz Chenomx™ database of small molecules (Chenomx NMR Suite 7.0, 2010; Wishart, 2008). Figure 3A illustrates an example of NMR spectral pattern peak fitting used to match the experimental spectra to a specific metabolite pattern (in this case, glucose) included in the reference spectrum of the Chenomx database. A comparison of overall spectral intensities of the different samples shows, based on normalized amounts of cell material (see material and methods section), that the overall spectral intensity of the *I. hospitalis-N-equitans* co-culture samples is generally less than that of the *I. hospitalis*-only samples. Eighteen of the 20 common amino acids, energy-related molecules like ADP, and nucleotides identified by NMR were found to be higher in concentration in the *I. hospitalis* grown alone samples compared to *I. hospitalis* grown in co-culture with *N. equitans*. Columns four and five of Table 1 list metabolites identified by NMR. As with the LC-MS metabolite data, a positive fold change indicates higher concentration when *I. hospitalis* is grown alone, and a negative fold change indicates higher concentration when *I. hospitalis* is grown in co-culture with *N. equitans*. Figure 3B shows a close-up of overlaid NMR spectra of *I. hospitalis* (black) alone and co-culture (red); arrows highlight NMR signals that are higher in intensity in the *I. hospitalis* alone samples or more intense in the *I. hospitalis-N-equitans* co-culture samples.

Integration of LC-MS and NMR Metabolic Profiling

Metabolomics, one of the more recent “omics” additions to Systems Biology research, is increasingly used to enhance our global understanding of complex biological systems and the impact of environment and pressure on the biological responses and adaptation of organisms. At present, most metabolomics research employs either nuclear magnetic

resonance (NMR) or mass spectrometry (MS), but rarely both. An important challenge in metabolomics is that a large fraction of the metabolites whose concentrations vary with alterations in biological conditions cannot be identified reliably using MS or NMR alone. NMR spectroscopy is very well suited for metabolomic analysis because a large number of small molecules can be assayed simultaneously in highly quantitative and reproducible manners. MS enables the analysis of a wide variety of compounds with excellent sensitivity. Using NMR and MS in concert enhances metabolic coverage and enables stronger identifications of key metabolic pathway components. Herein, integrating NMR and MS together has enabled to double the number of metabolites identified in *Ignicococcus hospitalis* only and *I. hospitalis – Nanoarcheum equitans* co-cultures. The integrated NMR and MS metabolomics approach has been crucial for this study as growth of these two archaea is extremely difficult and sample availability is limited.

Overall, the LC-MS and NMR data analyses were highly complementary. The LC-MS-based approach was able to identify metabolites present at low concentrations, while metabolite profiling by NMR resulted in the confident identification and accurate concentrations of each NMR identified metabolite (~ 35 metabolites). Fifteen compounds were identified by both LC-MS and NMR, with comparable fold changes measured by both methods for almost all of these compounds. There were also cases where one method could not obtain a reliable fold difference between *I. hospitalis* alone and the *I. hospitalis – N. equitans* co-cultures, due to low metabolite signal intensity or overlapping spectral peaks, but the complementary method could. There were also cases (see L-Proline or L-Pyroglutamate for examples) in which the ability to confirm the presence of a metabolite by both methods was extremely helpful. In combination, nearly 70 metabolites were identified with the two techniques, clearly demonstrating the power of using both LC-MS and NMR for metabolomics profiling of challenging systems such as these two archaea.

Metabolic Pathway Analysis of LC-MS and NMR Metabolomics Data

The LC-MS and NMR metabolic profiles were analyzed in the context of annotated metabolic pathways for *I. hospitalis* and *N. equitans* and current understanding of cellular events regulating these species' interactions. Using the Pathway Tools program, protein abundance data from a recent proteomics study and the metabolites identified in this study, integrated changes were mapped onto known biochemical pathways of *I. hospitalis and N. equitans* (Karp & Paley, 1996; Karp *et al*., 2005, 2010, 2002; Podar *et al*., 2008). This approach produced a global, system-wide analysis of metabolic networks that seem to be guiding cellular interactions between these two organisms. The resulting metabolic network map showed overlap and complementarity of proteomic and metabolomic datasets in several key pathways including arginine biosynthesis, CTP/UTP biosynthesis, and nutrient recycling (Figure 4). Although other amino acid pathways were altered by the presence of *N. equitans*, a strong correlation between proteomic and metabolomics data was specifically observed for arginine and isoleucine biosynthesis, warranting further analysis of such metabolic networks.

Interestingly, the biosynthetic pathway for arginine is up-regulated in the co-culture. Separate pathways important for arginine biosynthesis converge at ornithine carboxylase,

which produces citrulline from carbamoyl-phosphate and ornithine (Figure 4A). Citrulline is then converted to arginine in two steps involving arginosuccinate synthase and lyase enzymes. Proteomic analysis of the pathway showed increased abundance of carbamoyl phosphate synthase, ornithine carboxylase, and arginosuccinate lyase when *N. equitans* was present (Giannone *et al*., 2014). Metabolite data was consistent with increased flux through the pathway, as the intermediates ornithine and citrulline decreased whereas the end product arginine increased in abundance in the presence of *N. equitans*. Further investigation of the proteomics data revealed that enzymes producing ornithine were down regulated when *N. equitans* is present. This provides a rationale as to why ornithine dropped nearly 4-fold while arginine increased only 2-fold in the *I. hospitalis-N. equitans* co-cultures. This suggests that when *N. equitans* is present, the synthesis of arginine is largely accomplished through the consumption of available ornithine rather than by up-regulating enzymes needed to synthesize more ornithine. There are no other annotated pathways in *I. hospitalis* or *N. equitans* for which ornithine is a substrate, strongly suggesting that arginine biosynthesis leads to the decrease in ornithine. Together, the data imply that the interactions of *I. hospitalis* with *N. equitans* lead to induction of arginine synthesis at a low metabolic cost. This could be an important energy conservation mode, given the energetically depleted natural environment of these organisms and the resulting reduced strain on the energy balance of *I. hospitalis* (Thauer *et al*., 1977). Lysine, another basic amino acid, is less costly to synthesize in terms of ATP required, and a larger increase in concentration was observed in the co-culture. The higher abundance of lysine in the *I. hospitalis-N. equitans* co-cultures is consistent with the amino acid needs of proteins in *N. equitans* which have enriched lysine while lower arginine content (Podar *et al*., 2008).

Metabolite analysis indicated that the intracellular pool of amino acids was reduced in the presence of *N. equitans*. At the level of the proteome, the response is less clear (Giannone et al., 2014). While up regulation of amino acid and protein synthetic pathways in the *I. hospitalis* host does not seem to be required to sustain *N. equitans* growth, specific anabolic pathways such as those for branched chain amino acids and their backup intracellular importer systems actually decreased in abundance in the co-culture systems (Giannone et al. 2014). This suggests that sufficient amounts of amino acids exist in the cellular pool of *I. hospitalis* to meet the protein needs of *N. equitans*. Based on carefully conducted cell counts as reported in Giannone et al. 2014 (see their Figure 1A), the *I. hospitalis-N equitans* co-cultures used for the metabolomics studies contain approximately two *N. equitans* per *I. hospitalis.* At this ratio, only 2% of the total cell mass is *N. equitans*. Using the reported protein concentration for prokaryotes of 100 mg/mL as established by NMR, the total protein content of *N. equitans* is estimated to be about half of what is lost from the *I. hospitalis* host (Moran *et al*., 2010). Therefore, *I. hospitalis* would be expected to support growth of *N. equitans* through late-log phase without the need to synthesize *de novo* additional amino acids as a supply of amino acid precursors for *N. equitans* protein synthesis.

Based on the convergence of proteomic and metabolomics data, another pathway of particular interest was cytidine triphosphate (CTP) synthesis. This pathway is also energy intensive, involving the expenditure of three equivalents of adenosine triphosphate (ATP) to

make one CTP (Figure 4B). Many of the proteins and metabolites in this pathway, as well as the upstream pathway for uridine monophosphate (UMP) biosynthesis, showed significantly lower abundance in the *I. hospitalis-N. equitans* co-culture samples. CTP is essential for the synthesis of the archaeal lipid, archaeol (Boucher *et al*., 2004). Cytidine monophosphate was found by LC-MS to be at a higher concentration in *I. hospitalis* grown alone. From the observed depletion of CMP levels in the *I. hospitalis – N. equitans* co-cultures, we infer that CMP is converted to CTP to a greater extent in the *I. hospitalis – N. equitans* co-cultures, perhaps to be used for the biosynthesis of membrane archaeol lipids. During lipid synthesis, CTP becomes linked to the glycerol backbone of archaeol, forming CDP-archaeol (Boucher *et al*., 2004). The resulting lipid is then saturated by action of the enzyme geranyl-geranyl reductase, generating the active form of the lipid to be incorporated into cellular membranes.

The proteomics and metabolomics analyses together reveal a scenario revolving around *N. equitans*'s use of metabolites generated by *I. hospitalis* as a source of energy rather than for biomass production. To further explore this hypothesis, ATP, ADP, and AMP levels were measured in both *I. hospitalis* only and *I. hospitalis-N. equitans* co-cultures. Table 1 indicates that both LC-MS and NMR were able to identify AMP, and that NMR was also able to identify ADP. AMP was found to be in higher concentrations in the *I. hospitalis* only cultures, while ADP was found to be in a higher concentration in the co-culture. To quantify the ATP levels, a firefly luciferase assay was carried out. ATP was reproducibly measured to be at higher concentration when *I. hospitalis* is grown without *N. equitans* (Figure 5). The fact that ATP (high energy) and AMP (low energy) concentrations are in greater concentrations when *I. hospitalis* is grown alone, while the intermediate energy molecule ADP is higher in concentration in the *I. hospitalis-N. equitans* co-cultures suggests that there exists a significant energy demand for organism growth in the co-cultures. The trend of having more spent energy molecules (ADP) in the co-culture supports the notion that this additional energy demand placed upon *I. hospitalis* is necessary for growth of *N.* equitans and survival of its host *I. hospitalis* when the two species are grown together in co-cultures. To satisfy the increase in energy demand, the response of *I. hospitalis* to the presence of *N. equitans* seems to be to increase ATP production. The analysis was specifically presented in relative terms to normalize for possible degradation of nucleotide phosphate molecules due to the challenges of quenching samples grown at high temperature under hydrogen atmosphere.

Results from the luciferase assay suggested that the presence of *N. equitans* leads to increased ATP turnover. Some of this energy would likely be used to produce CTP, as suggested by the metabolic pathway analysis described above. This is supported by NMR metabolite profiling data which showed that the nucleotide bases (specifically cytidine and uridine) are higher in concentration in the *I. hospitalis-N. equitans* co-cultures, compared to the *I. hospitalis* only cultures. These results further support the notion that lipid production by *I. hospitalis* relies on available CTP levels, which originate from UMP biosynthesis as well as directly from cytidine metabolism.

Integration of results from proteomics and metabolomics experiments into a global scale analysis of metabolic pathways and networks of the combined cellular potential of these two organisms suggests that *N. equitans* exhibits parasitic function, not only consuming

metabolites for energy production but also using *I. hospitalis* to build important structural and cellular components such as membrane lipids. Both LC-MS and NMR analyses have noted a large decrease in the overall intracellular metabolite pool when the two organisms are grown together, indicating that *N. equitans* stimulates the consumption of intracellular metabolites of *I. hospitalis*. Further analysis of the energy status of these cells demonstrates that the presence of *N. equitans* depletes high energy nucleotide (ATP) concentrations, and shifts the energy potential to a lower energy state as indicated by the increased concentrations of ADP in the *I. hospitalis – N. equitans* co-cultures.

Biological Significance of the LC-MS and NMR Metabolomics Data

As noted above, both NMR and LC-MS metabolomics showed a decrease in abundance of most metabolites in the co-culture samples. Lower amino acid concentrations in the *I. hospitalis – N equitans* co-cultures suggest that those metabolites are utilized by *N. equitans* for protein biosynthesis, catabolized for energy production, or likely a combination of both. From this standpoint, it would suggest that *N. equitans*, as a user of *I. hospitalis* metabolic resources, may be acting more as a parasite rather than a mutualist with respect to metabolic needs of *I. hospitalis*. However, the question remains as to whether *I. hospitalis* could benefit from interactions with *N. equitans*, as many of the metabolic networks for these two organisms remain to be deciphered. For example, identification of maltotriose and stachyose as significant *I. hospitalis* metabolites suggest that *I. hospitalis* may be capable of more complex carbohydrate metabolism than has been anticipated. The LC-MS data on carbohydrate intermediates suggest that glucose or other carbohydrate storage pathways may be present in *I. hospitalis*, and could serve to maintain proper cellular osmotic control as well as to satisfy other metabolic needs.

Conclusion

This study is the first metabolomics analysis of the *I. hospitalis* and *N. equitans* interaction. This work also emphasizes the benefits of using both LC-MS and NMR approaches, as more complete characterization of the metabolome of *I. hospitalis* and *N. equitans* was obtained. Through integration of our LC-MS and NMR metabolite profiles with previously published proteomics data, we have been able to map several key metabolic pathways that appear to modulate *I. hospitalis-N equitans* interspecies interactions. This study has highlighted key metabolic changes occurring when *I. hospitalis* is grown in co-culture with *N. equitans*. Although *I. hospitalis* is able to grow in the presence of *N. equitans*, our data suggests that there is a significant metabolic cost for the host organism. *N. equitans* seems to consume a large fraction of the small molecule pool of *I. hospitalis*, producing a sharp decrease in the energy status of the host. We cannot rule out that in their natural environment, the interactions between these two organisms with severely reduced genomes may confer an ecological advantage in the larger meta-microbial community, but the results of this study suggest that, at least under the laboratory conditions used here, *N. equitans* imposes a significant metabolic energy strain on *I. hospitalis*. The combination of NMR and MS for untargeted metabolomics analysis has proven to be very powerful and complementary. Often times, the two methods yielded similar metabolite identification with comparable fold change measured by both for the different *I. hospitalis* and *I. hospitalis – N equitan*s

samples. In some cases, metabolite identification was only possible using either LC-MS or NMR but not both, making the use of both analytical platforms a necessity. Furthermore, the additional sensitivity of LC-MS for low abundance molecules combined with the ability of NMR to obtain quantitative metabolite concentrations (as opposed to relative concentrations) demonstrate the highly advantageous application of both techniques to untargeted metabolite profiling of challenging microbial systems.

Supplementary Material

Refer to Web version on PubMed Central for supplementary material.

Acknowledgments

Acknowledgment of financial support.

This research was supported by a grant from the U.S. Department of Energy, Office of Biological and Environmental Research (DE-SC0006654). The NMR experiments were recorded at Montana State University on a DRX600 Bruker solution NMR spectrometer, purchased in part with funds from the NIH Shared Instrumentation Grant (SIG) (Grant Number 1S10-RR13878-01), and recently upgraded to an AVANCE III console and cryogenically cooled TCI probe (Grant Number 1S10-RR026659-01). The mass spectrometry facility at MSU receives funding from the Murdock Charitable Trust and NIH 5P20RR02437 of the CoBRE program. We thank Dr. Harald Huber (University of Regensburg, Germany) for providing a bioreactor sample of *I. hospitalis-N. equitans* used for initial methods development.

References

Boucher Y, Kamekura M, Doolittle WF. Origins and evolution of isoprenoid lipid biosynthesis in archaea. Molecular Microbiology. 2004; 52(2):515–527.10.1111/j.1365-2958.2004.03992.x [PubMed: 15066037]

Burghardt T, Junglas B, Siedler F, Wirth R, Huber H, Rachel R. The interaction of Nanoarchaeum equitans with Ignicoccus hospitalis: proteins in the contact site between two cells. Biochemical Society Transactions. 2009; 37:127–32.10.1042/BST0370127 [PubMed: 19143616]

Chenomx NMR Suite 7.0. Chenomx Inc; 2010.

Giannone RJ, Huber H, Karpinets T, Heimerl T, Küper U, Rachel R, et al. Proteomic characterization of cellular and molecular processes that enable the Nanoarchaeum equitans--Ignicoccus hospitalis relationship. PloS one. 2011; 6(8):e22942.10.1371/journal.pone.0022942 [PubMed: 21826220]

Giannone RJ, Wurch LL, Heimerl T, Martin S, Yang Z, Huber H, Reinhard R, Hettich RL, Podar M. Life on the edge: functional genomic response of Ignicoccus hospitalis to the presence of Nanoarchaeum equitans. The ISME Journal. 2014 Jul 11.:1–14. Epub ahead of print. 10.1038/ismej.2014.112

Godde JS. Breaking through a phylogenetic impasse: a pair of associated archaea might have played host in the endosymbiotic origin of eukaryotes. Cell & Bioscience. 2012; 2:29, 1–11.10.1186/2045-3701-2-29 [PubMed: 22913376]

Heinemann J, Hamerly T, Maaty WS, Movahed N, Steffens JD, Reeves BD, et al. Expanding the paradigm of thiol redox in the thermophilic root of life. Biochimica et Biophysica Acta. 2014; 1840(1):80–85.10.1016/j.bbagen.2013.08.009 [PubMed: 23962628]

Huber H, Burggraf S, Mayer T, Wyschkony I, Rachel R, Stetter KO. Ignicoccus gen. nov., a novel genus of hyperthermophilic, chemolithoautotrophic Archaea, represented by two new species, Ignicoccus islandicus sp nov and Ignicoccus pacificus sp nov. and Ignicoccus pacificus sp. nov. International Journal of Systematic and Evolutionary Microbiology. 2000; 50:2093–2100. Retrieved from http://www.ncbi.nlm.nih.gov/pubmed/11155984. [PubMed: 11155984]

Huber H, Gallenberger M, Jahn U, Eylert E, Berg Ia, Kockelkorn D, et al. A dicarboxylate/4-hydroxybutyrate autotrophic carbon assimilation cycle in the hyperthermophilic Archaeum

Ignicoccus hospitalis. Proceedings of the National Academy of Sciences of the United States of America. 2008; 105(22):7851–7856.10.1073/pnas.0801043105 [PubMed: 18511565]

Huber H, Hohn MJ, Rachel R, Fuchs T, Wimmer VC, Stetter KO. A new phylum of Archaea represented by a nanosized hyperthermophilic symbiont. Nature. 2002; 417(6884):63–67.10.1038/417063a [PubMed: 11986665]

Huber H, Hohn MJ, Stetter KO, Rachel R. The phylum Nanoarchaeota: present knowledge and future perspectives of a unique form of life. Research in Microbiology. 2003; 154(3):165–171.10.1016/S0923-2508(03)00035-4 [PubMed: 12706504]

Huber H, Küper U, Daxer S, Rachel R. The unusual cell biology of the hyperthermophilic Crenarchaeon Ignicoccus hospitalis. Antonie van Leeuwenhoek. 2012; 102:203–219.10.1007/s10482-012-9748-5 [PubMed: 22653377]

Jahn U, Gallenberger M, Paper W, Junglas B, Eisenreich W, Stetter KO, et al. Nanoarchaeum equitans and Ignicoccus hospitalis: new insights into a unique, intimate association of two archaea. Journal of Bacteriology. 2008; 190(5):1743–1750.10.1128/JB.01731-07 [PubMed: 18165302]

Jahn U, Huber H, Eisenreich W, Hügler M, Fuchs G. Insights into the autotrophic CO2 fixation pathway of the archaeon Ignicoccus hospitalis: comprehensive analysis of the central carbon metabolism. Journal of Bacteriology. 2007; 189(11):4108–4119.10.1128/JB.00047-07 [PubMed: 17400748]

Jahn U, Summons R, Sturt H, Grosjean E, Huber H. Composition of the lipids of Nanoarchaeum equitans and their origin from its host Ignicoccus sp. strain KIN4/I. Archives of Microbiology. 2004; 182:404–413.10.1007/s00203-004-0725-x [PubMed: 15492905]

Junglas B, Briegel A, Burghardt T, Walther P, Wirth R, Huber H, Rachel R. Ignicoccus hospitalis and Nanoarchaeum equitans: ultrastructure, cell-cell interaction, and 3D reconstruction from serial sections of freeze-substituted cells and by electron cryotomography. Archives of Microbiology. 2008; 190:395–408.10.1007/s00203-008-0402-6 [PubMed: 18622597]

Karp PD, Ouzounis Ca, Moore-Kochlacs C, Goldovsky L, Kaipa P, Ahrén D, et al. Expansion of the BioCyc Collection of Pathway/Genome Databases to 160 Genomes. Nucleic Acids Research. 2005; 33(19):6083–6089.10.1093/nar/gki892 [PubMed: 16246909]

Karp PD, Paley S. Integrated Access to Metabolic and Genomic Data. Journal of Computational Biology. 1996; 3(1):191–212. Retrieved from http://www.ncbi.nlm.nih.gov/pubmed/8697237. [PubMed: 8697237]

Karp PD, Paley SM, Krummenacker M, Latendresse M, Dale JM, Lee TJ, et al. Pathway Tools version 13.0: Integrated Software for Pathway/Genome Informatics and Systems Biology. Briefings In Bioinformatics. 2010; 11(1):40–79.10.1093/bib/bbp043 [PubMed: 19955237]

Karp PD, Paley S, Romero P. The Pathway Tools Software. Bioinformatics. 2002; 18:S1–8.

Küper U, Meyer C, Müller V, Rachel R, Huber H. Energized outer membrane and spatial separation of metabolic processes in the hyperthermophilic Archaeon Ignicoccus hospitalis. Proceedings of the National Academy of Sciences of the United States of America. 2010; 107(7):3152–3156.10.1073/pnas.0911711107 [PubMed: 20133662]

Moran U, Phillips R, Milo R. SnapShot: key numbers in biology. Cell. 2010; 141(7):1262–1262.e1.10.1016/j.cell.2010.06.019 [PubMed: 20603006]

Paley SM, Latendresse M, Karp PD. Regulatory network operations in the Pathway Tools software. BMC Bioinformatics. 2012; 13:243.10.1186/1471-2105-13-243 [PubMed: 22998532]

Paper W, Jahn U, Hohn MJ, Kronner M, Näther DJ, Burghardt T, et al. Ignicoccus hospitalis sp. nov., the host of “Nanoarchaeum equitans”. International Journal of Systematic and Evolutionary Microbiology. 2007; 57:803–808.10.1099/ijs.0.64721-0 [PubMed: 17392210]

Podar M, Anderson I, Makarova KS, Elkins JG, Ivanova N, Wall MA, et al. A genomic analysis of the archaeal system Ignicoccus hospitalis-Nanoarchaeum equitans. Genome Biology. 2008; 9:R158.10.1186/gb-2008-9-11-r158 [PubMed: 19000309]

Promega Corporation. BacTiter-Glo Microbial Cell Viability Assay. 2012.

Sun J, Zhang S, Chen J, Han B. Metabolic profiling of Staphylococcus aureus cultivated under aerobic and anaerobic conditions with 1 H NMR-based nontargeted analysis. Canadian Journal of Microbiology. 2012; 718(17):709–718.10.1139/W2012-046 [PubMed: 22571732]

Thauer RK, Jungermann K, Decker K. Energy conservation in chemotrophic anaerobic bacteria. Bacteriology Reviews. 1977; 41(1):100–180.

Tredwell GD, Edwards-Jones B, Leak DJ, Bundy JG. The development of metabolomic sampling procedures for Pichia pastoris, and baseline metabolome data. PloS one. 2011; 6(1):e16286.10.1371/journal.pone.0016286 [PubMed: 21283710]

Waters E, Hohn MJ, Ahel I, Graham DE, Adams MD, Barnstead M, et al. The genome of Nanoarchaeum equitans: insights into early archaeal evolution and derived parasitism. Proceedings of the National Academy of Sciences of the United States of America. 2003; 100(22):12984–12988.10.1073/pnas.1735403100 [PubMed: 14566062]

Weljie AM, Newton J, Mercier P, Carlson E, Slupsky CM. Targeted profiling: quantitative analysis of 1H NMR metabolomics data. Analytical Chemistry. 2006; 78(13):4430–4442.10.1021/ac060209g [PubMed: 16808451]

Wishart DS. Quantitative metabolomics using NMR. Trends in Analytical Chemistry. 2008; 27(3): 228–237.10.1016/j.trac.2007.12.001

Wu X-H, Yu H-L, Ba Z-Y, Chen J-Y, And H-GS, Han B-Z. Sampling methods for NMR-based metabolomics of Staphylococcus aureus. Biotechnology Journal. 2010; 5(1):75–84. [PubMed: 19824021]

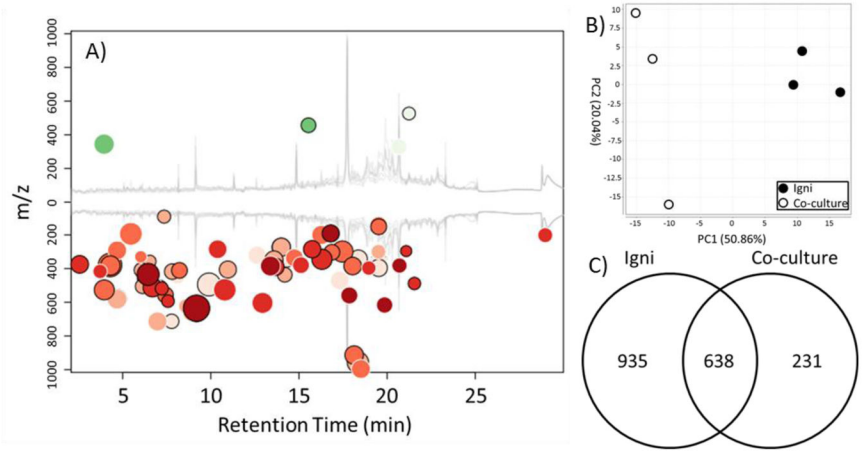

Figure 1. Analysis of metabolites by Reverse Phase LC-MS

(A) Cloud plot of extracted metabolites from *I. hospitalis* grown alone top, and co-culture of *I. hospitalis* and *N. equitans* bottom. Green circles denote a chromatographic peak whose mass spectral (MS) molecular feature is more abundant in the co-culture, and red circles denote a peak whose MS molecular feature is more abundant in *I. hospitalis* grown alone. The x-axis displays the retention/elution time of each molecular feature, while the y-axis indicates the m/z for each molecular feature. Only molecular features with a fold change greater than 1.5 and a p-value less than 0.01 are shown. (B) A 2D PCA score plot indicating the separation of biological triplicates for *I. hospitalis* and the *I. hospitalis-N equitans* co-culture. The co-culture exhibits more variance in PC2 than the *I. hospitalis* samples; this likely arises from the variability that *N. equitans* contributes when grown with *I. hospitalis* . (C) Venn diagram indicating the number of unique and shared MS molecular features found in each sample.

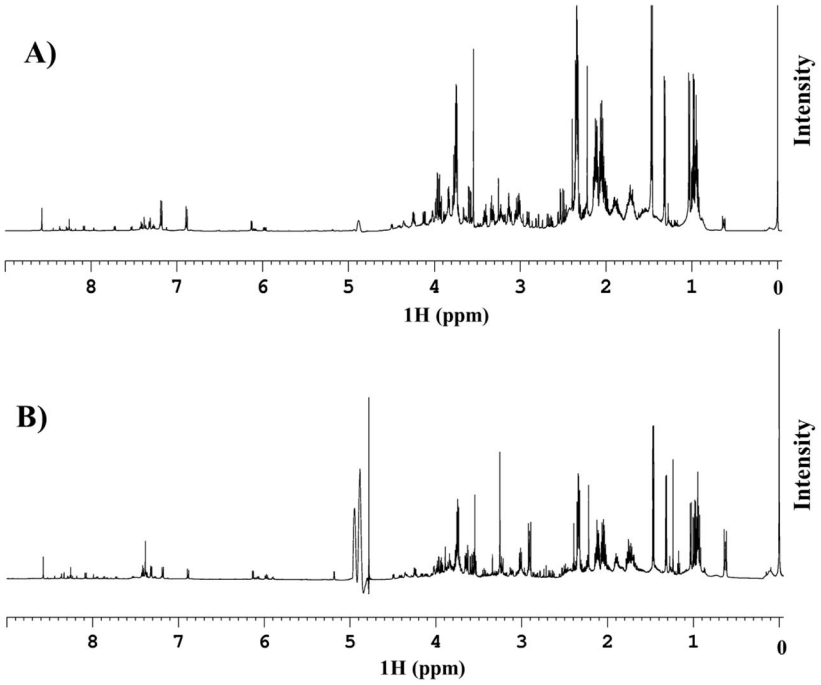

Figure 2.

Representative 1D ^{1}H NMR spectra corresponding to the intracellular metabolite profiles of (A) *I. hospitalis*-only cell cultures (B) and of *I. hospitalis – N. equitans* co-cultures normalized to total integrated spectral intensity of each spectrum.

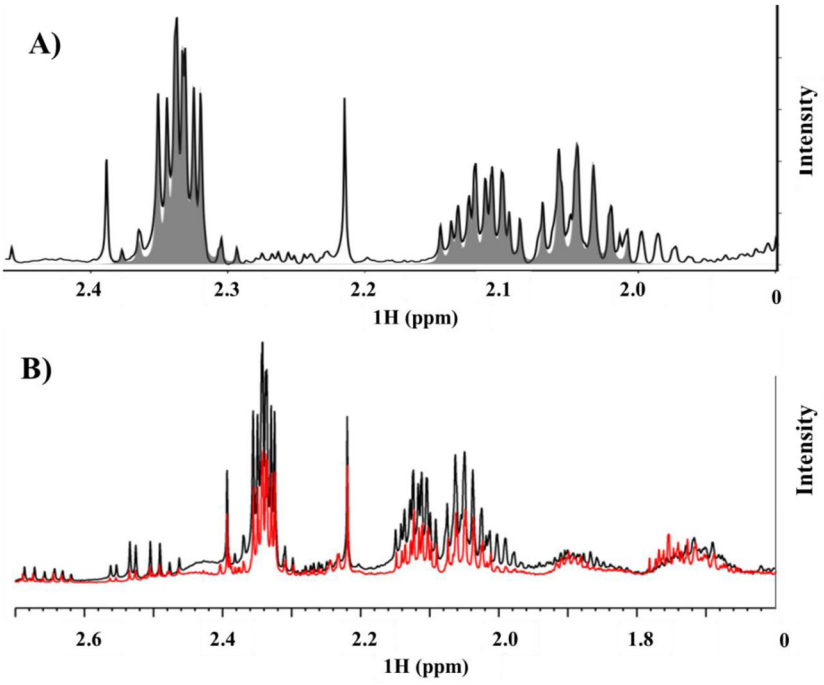

Figure 3.

(A) Expanded view of a section of the ^{1}H NMR spectrum originating from *Ignicoccus hospitalis*-only cell cultures spanning the ^{1}H chemical shift region 0 to 2.5 ppm, highlighting the spectral features and peak patterns corresponding to the metabolite glucose, as fitted (in grey) with the Chenomx NMR software.(B) Expanded view of a region of the ^{1}H NMR spectra of *I. hospitalis* (black spectrum) and *I. hospitalis-N equitans* co-culture (red spectrum) overlaid on top of each other and spanning the ^{1}H chemical shift region of 0 to 3 ppm. The black arrows highlight metabolite signals that are greater (right arrow) or lower (left arrow) in intensity in the *I. hospitalis-N. equitans* co-culture sample than the ones observed for the *I. hospitalis*-only sample, following normalization of spectral intensities (as described in the text)

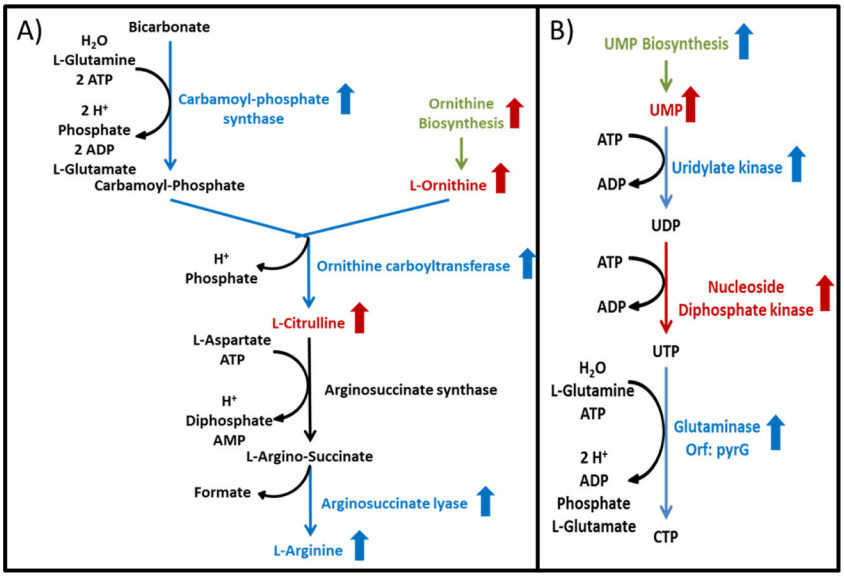

Figure 4. Schematics from Pathway Analysis

Overlay of proteomic and metabolomic analysis for two metabolic pathways: (A) arginine biosynthesis, and (B) CTP biosynthesis. Proteins and metabolites identified by proteomics and metabolomics experiments which displayed a fold change greater than 1.5 between cultures are highlighted in color; red indicates a greater concentration in the *I. hospitalis*-only culture, while blue indicates a greater concentration in the *I. hospitalis*-*N. equitans* co-culture.

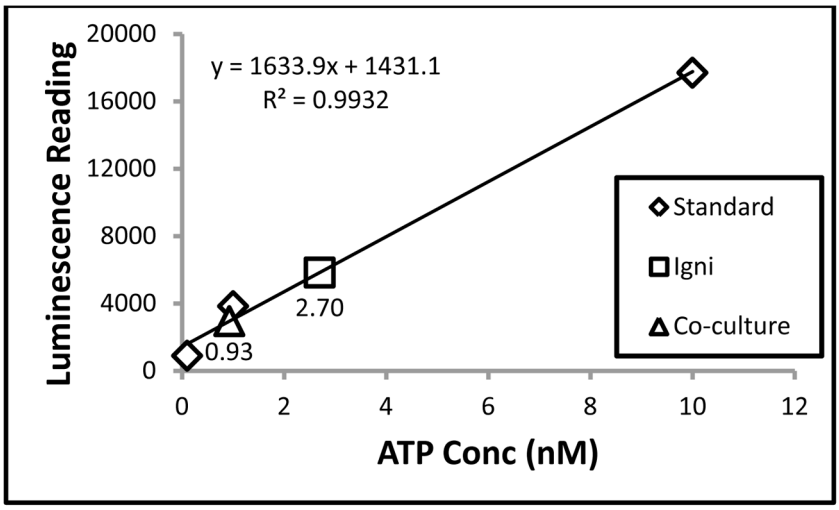

Figure 5. ATP concentration as measured from ATP Luciferase Assays

Standard curve generated from ATP Luciferase assays, with trend line and equation shown. Levels obtained for *I. hospitalis* grown alone (red square) and in co-culture with *N. equitans* (green triangle) are shown, with the calculated value of ATP shown below each respectively data point. Standard deviation for each data point was less than 2%.

Table 1

Metabolites identified by LC-MS and

	LC-MS				NMR
Metabolite	**Pwy**	**Std**	**Fold**	***p*-value**	**Fold**
(3S)-3,6-Diaminohexanoate	X		4.6	0.24	
2-Aminoadipate					NSC
2-Oxo-4-Methylthiobutanoate	X		*	-	
2-Oxoisocaproate					#
3-Methyl-2-oxovalerate					#
5,6-Dihydrothymine					*
5-Oxoproline	X		2.7	0.08	
Adenine	X		*	-	
Adenosine					−5.3
ADP					−2.3
Agmatine	X	X	2.8	0.22	*
AMP		X	8.8	0.07	1.7
Betaine					NSC
Butanal	X		−1.4	0.52	
Carnitine					#
CMP		X	3.2	0.19	
Cytidine					−10.9
Dimethyl sulfone					9.5
Dimethylamine					13.3
dTTP					−3.7
Formate					−2.5
Fumarate					*
Glucose					#
Glucuronamide		X	#	-	
Glycine					2.6
Guanosine					#

	LC-MS				NMR
Metabolite	**Pwy**	**Std**	**Fold**	***p*-value**	**Fold**
Hydroxymethylbilane	X		#	-	
Indole-3-acetate					−2.2
Inosine					−1.9
L-2-Aminoadipate	X		4.4	0.07	
Lactate					−1.8
L-Alanine					2.8
L-Arginine	X	X[1]	1.8	0.30	NSC
L-Asparagine					#
L-Aspartate	X	X	2.4	0.57	3.4
L-Aspartyl-4-Phosphate	X		#	-	
L-Citrulline	X	X	3.6	0.12	3.0
L-Glutamate	X	X	2.3	0.12	2.3
L-Histidine	X	X[1]	24.8	0.39	1.6
L-Homoserine	X	X[1]	6.9	0.01	
L-Isoleucine	X	X[1]	1.9	0.38	NSC
L-Leucine	X	X[1]	1.9	0.38	NSC
L-Lysine	X	X[1]	4.6	0.24	NSC
L-Methionine					1.9
L-Omithine					3.9
L-Phenylalanine	X		NSC		−2.0
L-Proline	X	X[1]	5.3	0.01	7.1
L-Pyroglutamate					#
L-Serine					2.5
L-Threonine	X	X[1]	6.9	0.01	1.5
L-Tryptophan					1.5
L-Tyrosine					2.0
L-Valine					1.5

	LC-MS				NMR
Metabolite	**Pwy**	**Std**	**Fold**	***p*-value**	**Fold**
Malonate					1.6
Maltotriose		X	#	-	
Menadione	X		2.4	0.09	
N2-Acetyl-L-Lysine	X		5.6	0.03	
N-Acetyl-L-Glutamate	X	X	6.5	0.01	
N-Acetyltyrosine					*
Nicotinate					−3.5
N-Isovaleroylglycine					#
O-Acetyl-L-Homoserine	X		4.4	0.07	
O-Succinyl-L-Homoserine	X		*	-	
Oxypurinol					#
Phenylethyl-amine		X	NSC		
Phytyl Diphosphate	X		#	-	
Propanal	X		-1.4	0.69	
Pseudouridine 5'-Phosphate	X		*	-	
Riboflavin	X		7.9	0.06	
S-Adenosyl-L-Homocysteine	X		*	-	−1.4
Stachyose		X	#	-	
Succinate					1.9
Trehalose					−6.6
Tyramine		X	NSC		
Tyrosol	X		1.5	0.15	
UDP-glucose					−2.2
UDP-N-Acetylglucosamine					−2.9
UMP					−1.7
Uracil					−6.6
Uridine					−5.9

Putatively metabolite IDs based on annotated pathways from Biocyc **(Pwy)**

Confirmed metabolite IDs based on MS standards **(Std)**

Metabolite IDs from spectral features of compounds identified by NMR **(NMR)**

Fold change between the *I. hospitalis* only samples and the *I. hospitalis – N equitans* co-culture, where a positive number indicates a higher concentration in the *I. hospitalis* only culture.

*denotes a compound seen only in the *I. hospitalis culture*

#denotes a compound seen only *when N. equitans* is present in the co-culture.

*1*denotes confirmed by MS/MS

NSC denotes No Significant Change

Metabolomics. Author manuscript; available in PMC 2016 August 01.